Cambridge University Press
978-1-107-00237-1 - Hydrodynamics of Pumps
Christopher E. Brennen
Excerpt
More information

1

Introduction

1.1 Subject

The subject of this monograph is the fluid dynamics of liquid turbomachines, particularly pumps. Rather than attempt a general treatise on turbomachines, we shall focus attention on those special problems and design issues associated with the flow of liquid through a rotating machine. There are two characteristics of a liquid that lead to these special problems, and cause a significantly different set of concerns than would occur in, say, a gas turbine. These are the potential for cavitation and the high density of liquids that enhances the possibility of damaging unsteady flows and forces.

1.2 Cavitation

The word cavitation refers to the formation of vapor bubbles in regions of low pressure within the flow field of a liquid. In some respects, cavitation is similar to boiling, except that the latter is generally considered to occur as a result of an increase of temperature rather than a decrease of pressure. This difference in the direction of the state change in the phase diagram is more significant than might, at first sight, be imagined. It is virtually impossible to cause any rapid uniform change in temperature throughout a finite volume of liquid. Rather, temperature change most often occurs by heat transfer through a solid boundary. Hence, the details of the boiling process generally embrace the detailed interaction of vapor bubbles with a solid surface, and the thermal boundary layer on that surface. On the other hand, a rapid, uniform change in pressure in a liquid is commonplace and, therefore, the details of the cavitation process may differ considerably from those that occur in boiling. Much more detail on the process of cavitation is included in later sections.

It is sufficient at this juncture to observe that cavitation is generally a malevolent process, and that the deleterious consequences can be divided into three categories. First, cavitation can cause damage to the material surfaces close to the area where the bubbles collapse when they are convected into regions of higher pressure. Cavitation damage can be very expensive, and very difficult to eliminate. For most designers of hydraulic machinery, it is the preeminent problem associated with cavitation. Frequently, one begins with the objective of eliminating cavitation completely. However, there are many circumstances in which this proves to be impossible, and the effort must be redirected into minimizing the adverse consequences of the phenomenon.

The second adverse effect of cavitation is that the performance of the pump, or other hydraulic device, may be significantly degraded. In the case of pumps, there is generally a level of inlet pressure at which the performance will decline dramatically, a phenomenon termed cavitation breakdown. This adverse effect has naturally given rise to changes in the design of a pump so as to minimize the degradation of the performance; or, to put it another way, to optimize the performance in the presence of cavitation. One such design modification is the addition of a cavitating inducer upstream of the inlet to a centrifugal or mixed flow pump impeller. Another example is manifest in the blade profiles used for supercavitating propellers. These supercavitating hydrofoil sections have a sharp leading edge, and are shaped like curved wedges with a thick, blunt trailing edge.

The third adverse effect of cavitation is less well known, and is a consequence of the fact that cavitation affects not only the steady state fluid flow, but also the unsteady or dynamic response of the flow. This change in the dynamic performance leads to instabilities in the flow that do not occur in the absence of cavitation. Examples of these instabilities are "rotating cavitation," which is somewhat similar to the phenomenon of rotating stall in a compressor, and "auto-oscillation," which is somewhat similar to compressor surge. These instabilities can give rise to oscillating flow rates and pressures that can threaten the structural integrity of the pump or its inlet or discharge ducts. While a complete classification of the various types of unsteady flow arising from cavitation has yet to be constructed, we can, nevertheless, identify a number of specific types of instability, and these are reviewed in later chapters of this monograph.

1.3 Unsteady Flows

While it is true that cavitation introduces a special set of fluid-structure interaction issues, it is also true that there are many such unsteady flow problems which can arise even in the absence of cavitation. One reason these issues may be more critical in a liquid turbomachine is that the large density of a liquid implies much larger fluid dynamic forces. Typically, fluid dynamic forces scale like $\rho\Omega^2 D^4$ where ρ is the fluid density, and Ω and D are the typical frequency of rotation and the typical length, such as the span or chord of the impeller blades or the diameter of the impeller. These forces are applied to blades whose typical thickness is denoted by τ. It follows that the typical structural stresses in the blades are given by $\rho\Omega^2 D^4/\tau^2$, and, to minimize structural problems, this quantity will have an upper bound which will depend on the material. Clearly this limit will be more stringent when the density of the fluid is larger. In many pumps and liquid turbines it requires thicker blades (larger τ) than would be advisable from a purely hydrodynamic point of view.

This monograph presents a number of different unsteady flow problems that are of concern in the design of hydraulic pumps and turbines. For example, when a rotor blade passes through the wake of a stator blade (or vice versa), it will encounter an unsteady load which is endemic to all turbomachines. Recent investigations of these loads will be reviewed. This rotor-stator interaction problem is an example of a local unsteady flow phenomenon. There also exist global unsteady flow problems, such as the auto-oscillation problem mentioned earlier. Other global unsteady flow problems are caused by the fluid-induced radial loads on an impeller due to flow asymmetries, or the fluid-induced rotordynamic loads that may increase or decrease the critical whirling speeds of the shaft system. These last issues have only recently been addressed from a fundamental research perspective, and a summary of the conclusions is included in this monograph.

1.4 Trends in Hydraulic Turbomachinery

Though the constraints on a turbomachine design are as varied as the almost innumerable applications, there are a number of ubiquitous trends which allow us to draw some fairly general conclusions. To do so we make use of the affinity laws that are a consequence of dimensional analysis, and relate performance characteristics to the density of the fluid, ρ, the typical rotational speed, Ω, and the typical diameter, D, of the pump. Thus the volume flow rate through the pump, Q, the total head rise across the pump, H, the torque, T, and the power absorbed by the pump, P, will scale according to

$$Q \propto \Omega D^3 \tag{1.1}$$

$$H \propto \Omega^2 D^2 \tag{1.2}$$

$$T \propto \rho D^5 \Omega^2 \tag{1.3}$$

$$P \propto \rho D^5 \Omega^3 \tag{1.4}$$

These simple relations allow basic scaling predictions and initial design estimates. Furthermore, they permit consideration of optimal characteristics, such as the power density which, according to the above, should scale like $\rho D^2 \Omega^3$.

One typical consideration arising out of the affinity laws relates to optimizing the design of a pump for a particular power level, P, and a particular fluid, ρ. This fixes the value of $D^5 \Omega^3$. If one wished to make the pump as small as possible (small D) to reduce weight (as is critical in the rocket engine context) or to reduce cost, this would dictate not only a higher rotational speed, Ω, but also a higher impeller tip speed, $\Omega D/2$. However, as we shall see in the next chapter, the propensity for cavitation increases as a parameter called the cavitation number decreases, and the cavitation number is inversely proportional to the square of the tip speed or $\Omega^2 D^2/4$. Consequently, the increase in tip speed suggested above could lead to a cavitation problem. Often, therefore, one designs the smallest pump that will still operate without cavitation, and this implies a particular size and speed for the device.

Furthermore, as previously mentioned, the typical fluid-induced stresses in the structure will be given by $\rho\Omega^2 D^4/\tau^2$, and, if $D^5\Omega^3$ is fixed and if one maintains the same geometry, D/τ, then the stresses will increase like $D^{-4/3}$ as the size, D, is decreased. Consequently, fluid/structure interaction problems will increase. To counteract this the blades are often made thicker (D/τ is decreased), but this usually leads to a decrease in the hydraulic performance of the turbomachine. Consequently an optimal design often requires a balanced compromise between hydraulic and structural requirements. Rarely does one encounter a design in which this compromise is optimal.

Of course, the design of a pump, compressor or turbine involves many factors other than the technical issues discussed above. Many compromises and engineering judgments must be made based on constraints such as cost, reliability and the expected life of a machine. This book will not attempt to deal with such complex issues, but will simply focus on the advances in the technical data base associated with cavitation and unsteady flows. For a broader perspective on the design issues, the reader is referred to engineering texts such as those listed at the end of this chapter.

1.5 Book Structure

The intention of this monograph is to present an account of both the cavitation issues and the unsteady flow issues, in the hope that this will help in the design of more effective liquid turbomachines. In chapter 2 we review some of the basic principles of the fluid mechanical design of turbomachines for incompressible fluids, and follow that, in chapter 3, with a discussion of the two-dimensional performance analyses based on the flows through cascades of foils. A brief review of three-dimensional effects and secondary flows follows in chapter 4. Then, in chapter 5, we introduce the parameters which govern the phenomenon of cavitation, and describe the different forms which cavitation can take. This is followed by a discussion of the factors which influence the onset or inception of cavitation. Chapter 6 introduces concepts from the analyses of bubble dynamics, and relates those ideas to two of the byproducts of the phenomenon, cavitation damage and noise. The isssues associated with the performance of a pump under cavitating conditions are addressed in chapter 7.

The last three chapters deal with unsteady flows and vibration in pumps. Chapter 8 presents a survey of some of the vibration problems in pumps. Chapter 9 provides details of the two basic approaches to the analysis of instabilites and unsteady flow problems in hydraulic systems, namely the methods of solution in the time domain and in the frequency domain. Where possible, it includes a survey of the existing information on the dynamic response of pumps under cavitating and non-cavitating conditions. The final chapter 10 deals with the particular fluid/structure interactions associated with rotordynamic shaft vibrations, and elucidates the fluid-induced rotordynamic forces that can result from the flows through seals and through and around impellers.

Cambridge University Press
978-1-107-00237-1 - Hydrodynamics of Pumps
Christopher E. Brennen
Excerpt
More information

2

Basic Principles

2.1 Geometric Notation

The geometry of a generalized turbomachine rotor is sketched in figure 2.1, and consists of a set of rotor blades (number = Z_R) attached to a hub and operating within a static casing. The radii of the inlet blade tip, inlet blade hub, discharge blade tip, and discharge blade hub are denoted by R_{T1}, R_{H1}, R_{T2}, and R_{H2}, respectively. The discharge blade passage is inclined to the axis of rotation at an angle, ϑ, which would be close to 90° in the case of a centrifugal pump, and much smaller in the case of an axial flow machine. In practice, many pumps and turbines are of the "mixed flow" type, in which the typical or mean discharge flow is at some intermediate angle, $0 < \vartheta < 90°$.

The flow through a general rotor is normally visualized by developing a meridional surface (figure 2.2), that can either correspond to an axisymmetric streamsurface, or be some estimate thereof. On this meridional surface (see figure 2.2) the fluid velocity in a non-rotating coordinate system is denoted by $v(r)$ (with subscripts 1 and 2 denoting particular values at inlet and discharge) and the corresponding velocity relative to the rotating blades is denoted by $w(r)$. The velocities, v and w, have components v_θ and w_θ in the circumferential direction, and v_m and w_m in the meridional direction. Axial and radial components are denoted by the subscripts a and r. The velocity of the blades is Ωr. As shown in figure 2.2, the flow angle $\beta(r)$ is defined as the angle between the relative velocity vector in the meridional plane and a plane perpendicular to the axis of rotation. The blade angle $\beta_b(r)$ is defined as the inclination of the tangent to the blade in the meridional plane and the plane perpendicular to the axis of rotation. If the flow is precisely parallel to the blades, $\beta = \beta_b$. Specific values of the blade angle at the leading and trailing edges (1 and 2) and at the hub and tip (H and T) are denoted by the corresponding suffices, so that, for example, β_{bT2} is the blade angle at the discharge tip.

At the leading edge it is important to know the angle $\alpha(r)$ with which the flow meets the blades, and, as defined in figure 2.3,

$$\alpha(r) = \beta_{b1}(r) - \beta_1(r). \tag{2.1}$$

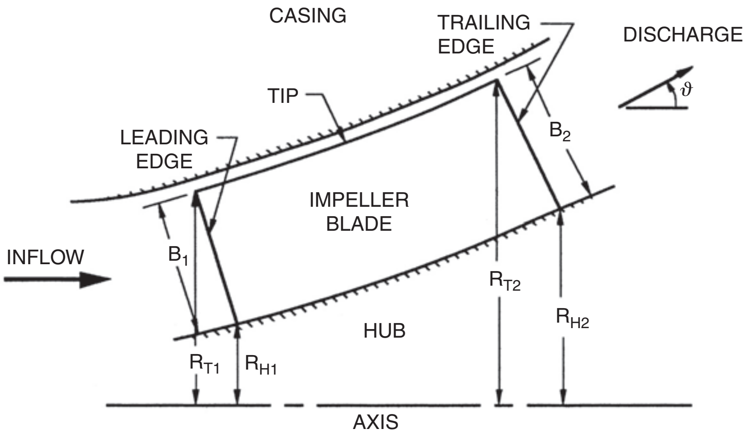

Figure 2.1. Cross-sectional view through the axis of a pump impeller.

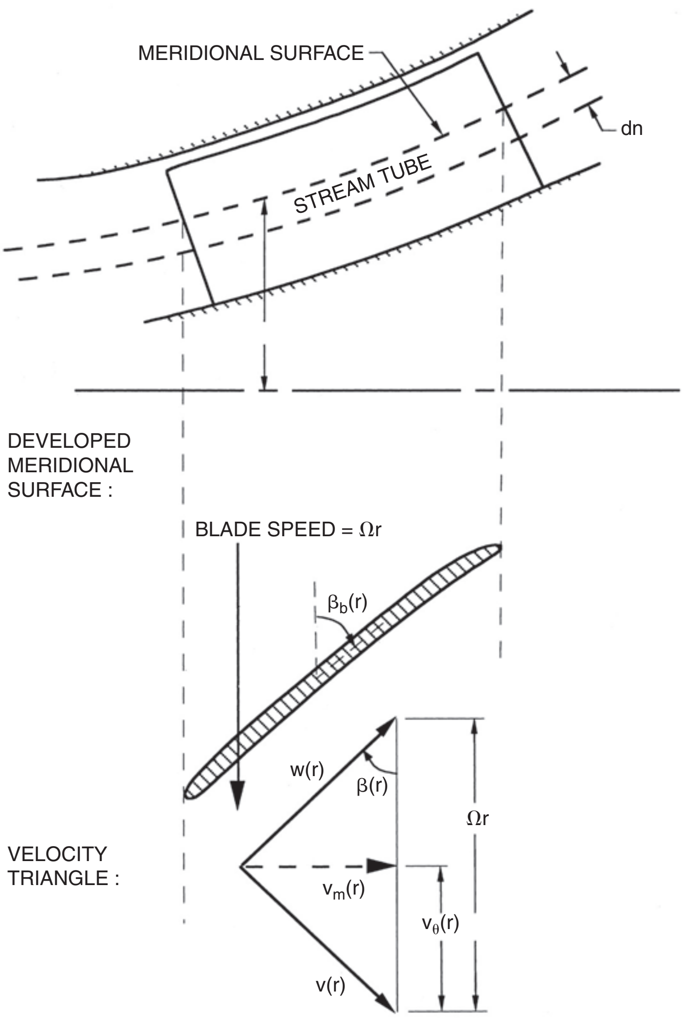

Figure 2.2. Developed meridional surface and velocity triangle.

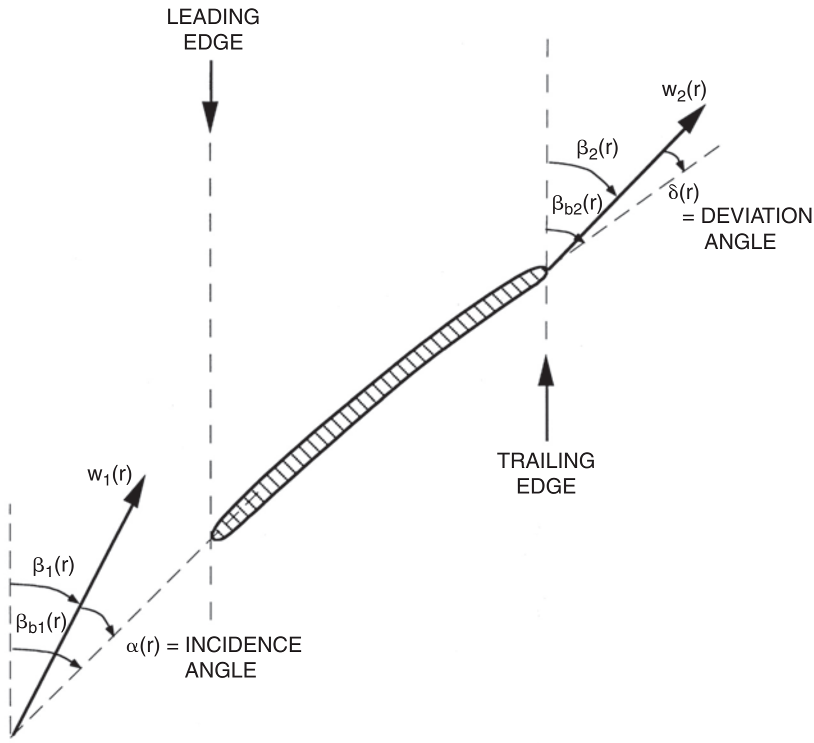

Figure 2.3. Repeat of figure 2.2 showing the definitions of the incidence angle at the leading edge and the deviation angle at the trailing edge.

This angle, α, is called the incidence angle, and, for simplicity, we shall denote the values of the incidence angle at the tip, $\alpha(R_{T1})$, and at the hub, $\alpha(R_{H1})$, by α_T and α_H, respectively. Since the inlet flow can often be assumed to be purely axial ($v_1(r) = v_{a1}$ and parallel with the axis of rotation), it follows that $\beta_1(r) = \tan^{-1}(v_{a1}/\Omega r)$, and this can be used in conjunction with equation 2.1 in evaluating the incidence angle for a given flow rate.

The incidence angle should not be confused with the "angle of attack," which is the angle between the incoming relative flow direction and the chord line (the line joining the leading edge to the trailing edge). Note, however, that, in an axial flow pump with straight helicoidal blades, the angle of attack is equal to the incidence angle.

At the trailing edge, the difference between the flow angle and the blade angle is again important. To a first approximation one often assumes that the flow is parallel to the blades, so that $\beta_2(r) = \beta_{b2}(r)$. A departure from this idealistic assumption is denoted by the deviation angle, $\delta(r)$, where, as shown in figure 2.3:

$$\delta(r) = \beta_{b2}(r) - \beta_2(r) \tag{2.2}$$

This is normally a function of the ratio of the width of the passage between the blades to the length of the same passage, a geometric parameter known as the solidity which is

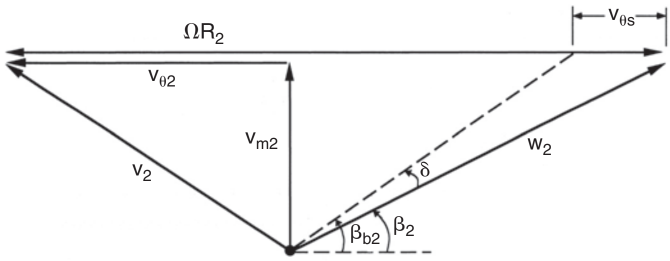

Figure 2.4. Velocity vectors at discharge indicating the slip velocity, $v_{\theta s}$.

defined more precisely below. Other angles, that are often used, are the angle through which the flow is turned, known as the *deflection angle*, $\beta_2 - \beta_1$, and the corresponding angle through which the blades have turned, known as the *camber angle* and denoted by $\theta_c = \beta_{b2} - \beta_{b1}$.

Deviation angles in radial machines are traditionally represented by the *slip velocity*, $v_{\theta s}$, which is the difference between the actual and ideal circumferential velocities of the discharge flow, as shown in figure 2.4. It follows that

$$v_{\theta s} = \Omega R_2 - v_{\theta 2} - v_{r2} \cot \beta_{b2} \tag{2.3}$$

This, in turn, is used to define a parameter known as the *slip factor*, Sf, where

$$Sf = 1 - \frac{v_{\theta s}}{\Omega R_2} = 1 - \phi_2 (\cot \beta_2 - \cot \beta_{b2}) \tag{2.4}$$

Other, slightly different "slip factors" have also been used in the literature; for example, Stodola (1927), who originated the concept, defined the slip factor as $1 - v_{\theta s} \big/ \Omega R_2 (1 - \phi_2 \cot \beta_{b2})$. However, the definition 2.4 is now widely used. It follows that the deviation angle, δ, and the slip factor, Sf, are related by

$$\delta = \beta_{b2} - \cot^{-1} \left(\cot \beta_{b2} + \frac{(1 - Sf)}{\phi_2} \right) \tag{2.5}$$

where the flow coefficient, ϕ_2, is defined later in equation 2.17.

2.2 Cascades

We now turn to some specific geometric features that occur frequently in discussions of pumps and other turbomachines. In a purely axial flow machine, the development of a cylindrical surface within the machine produces a *linear cascade* of the type shown in figure 2.5(a). The centerplane of the blades can be created using a "generator," say $z = z^*(r)$, which is a line in the rz–plane. If this line is rotated through a helical path, it describes a helicoidal surface of the form

$$z = z^*(r) + \frac{h_p \theta}{2\pi} \tag{2.6}$$

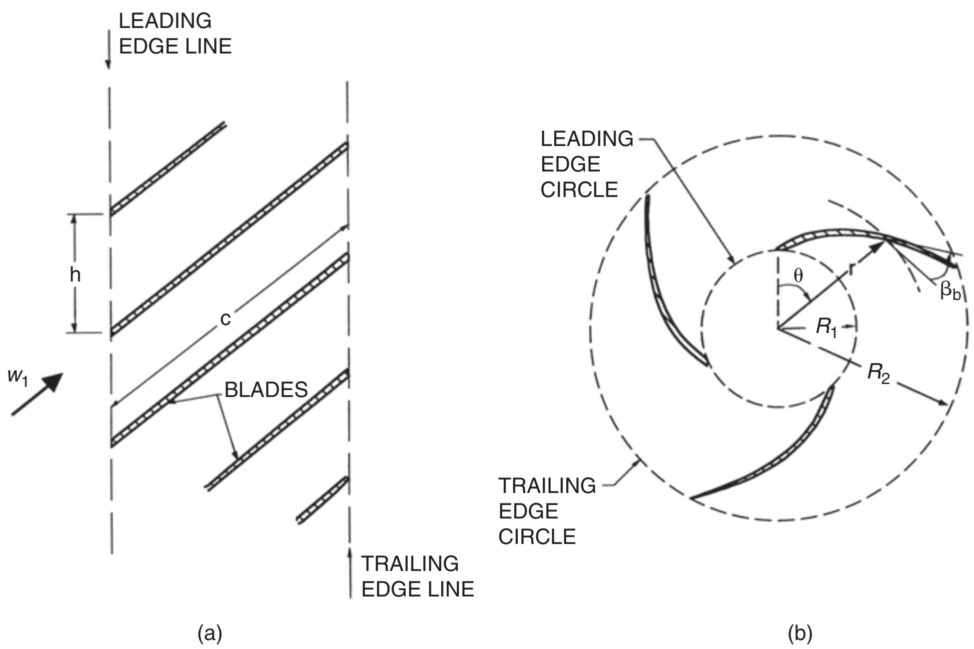

Figure 2.5. Schematics of (a) a linear cascade and (b) a radial cascade.

where h_p is the "pitch" of the helix. Of course, in many machines, the pitch is also a function of θ so that the flow is turned by the blades. If, however, the pitch is constant, the development of a cylindrical surface will yield a cascade with straight blades and constant blade angle, β_b. Moreover, the blade thickness is often neglected, and the blades in figure 2.5(a) then become infinitely thin lines. Such a cascade of infinitely thin, flat blades is referred to as a *flat plate cascade*.

It is convenient to use the term "simple" cascade to refer to those geometries for which the blade angle, β_b, is constant whether in an axial, radial, or mixed flow machine. Clearly, the flat plate cascade is the axial flow version of a simple cascade.

Now compare the geometries of the cascades at different radii within an axial flow machine. Later, we analyse the cavitating flow occurring at different radii (see figure 7.35). Often the pitch at a given axial position is the same at all radii. Then it follows that the radial variation in the blade angle, $\beta_b(r)$, must be given by

$$\beta_b(r) = \tan^{-1}\left[\frac{R_T \tan \beta_{bT}}{r}\right] \tag{2.7}$$

where β_{bT} is the blade angle at the tip, $r = R_T$.

In a centrifugal machine in which the flow is purely radial, a cross-section of the flow would be as shown in figure 2.5(b), an array known as a *radial cascade*. In a *simple* radial cascade, the angle, β_b, is uniform along the length of the blades. The resulting blade geometry is known as a logarithmic spiral, since it follows that the coordinates of the blades are given by the equation

$$\theta - \theta_0 = A\, ln\, r \tag{2.8}$$

where $A = \cot \beta_b$ and θ_0 are constants. Logarithmic spiral blades are therefore equivalent to straight blades in a linear cascade. Note that a fluid particle in a flow of uniform circulation and constant source strength at the origin will follow a logarithmic spiral since all velocities will be of the form C/r where C is a uniform constant.

In any of type of pump, the ratio of the length of a blade passage to its width is important in determining the degree to which the flow is guided by the blades. The solidity, s, is the geometric parameter that is used as a measure of this geometric characteristic, and s can be defined for any *simple* cascade as follows. If we identify the difference between the θ coordinates for the same point on adjacent blades (call this $\Delta\theta_A$) and the difference between the θ coordinates for the leading and trailing edges of a blade (call this $\Delta\theta_B$), then the solidity for a simple cascade is defined by

$$s = \frac{\Delta\theta_B}{\Delta\theta_A \cos\beta_b} \tag{2.9}$$

Applying this to the linear cascade of figure 2.5(a), we find the familiar

$$s = c/h \tag{2.10}$$

In an axial flow pump this corresponds to $s = Z_R c/2\pi R_{T1}$, where c is the chord of the blade measured in the developed meridional plane of the blade tips. On the other hand, for the radial cascade of figure 2.5(b), equation 2.9 yields the following expression for the solidity:

$$s = Z_R \ell n \left(R_2/R_1\right)/2\pi \sin\beta_b \tag{2.11}$$

which is, therefore, geometrically equivalent to c/h in the linear cascade.

In practice, there exist many "mixed flow" pumps whose geometries lie between that of an axial flow machine ($\vartheta = 0$, figure 2.1) and that of a radial machine ($\vartheta = \pi/2$). The most general analysis of such a pump would require a cascade geometry in which figures 2.5(a) and 2.5(b) were *projections* of the geometry of a meridional surface (figure 2.2) onto a cylindrical surface and onto a plane perpendicular to the axis, respectively. (Note that the β_b marked in figure 2.5(b) is not appropriate when that diagram is used as a projection). We shall not attempt such generality here; rather, we observe that the meridional surface in many machines is close to conical. Denoting the inclination of the cone to the axis by ϑ, we can use equation 2.9 to obtain an expression for the solidity of a simple cascade in this conical geometry,

$$s = Z_R \ell n \left(R_2/R_1\right)/2\pi \sin\beta_b \sin\vartheta \tag{2.12}$$

Clearly, this includes the expressions 2.10 and 2.11 as special cases.